JOURNAL OF APPLIED PHYSICS **108**, 013708 (2010)

Effect of threading screw and edge dislocations on transport properties of 4H–SiC homoepitaxial layers

S. I. Maximenko,[1,a)] J. A. Freitas, Jr.,[1] R. L. Myers-Ward,[1] K.-K. Lew,[1] B. L. VanMil,[1] C. R. Eddy, Jr.,[1] D. K. Gaskill,[1] P. G. Muzykov,[2] and T. S. Sudarshan[2]
[1]*Naval Research Laboratory, Washington, DC 20375, USA*
[2]*Department of Electrical Engineering, University of South Carolina, Columbia, South Carolina 29208, USA*

(Received 9 March 2010; accepted 13 May 2010; published online 8 July 2010)

Local recombination properties of threading screw and edge dislocations in 4H–SiC epitaxial layers have been studied using electron beam induced current (EBIC). The minority carrier diffusion length in the vicinity of dislocations was found to vary with dislocation type. Screw dislocations had a more pronounced impact on diffusion length than the edge dislocations, evidencing stronger recombination activity. Temperature dependence of EBIC contrast of dislocations suggests that their recombination activity is controlled by deep energy levels in the vicinity of dislocation cores. This paper shows that the type of dislocation (screw or edge) can be identified from analysis of EBIC contrast. © *2010 American Institute of Physics*. [doi:10.1063/1.3448230]

I. INTRODUCTION

For many years it has been known that dislocations introduce energy levels within the band gap, altering recombination properties of the surrounding semiconductor material. Shockley[1] was the first to suggest that dangling bonds in the dislocation core may act as traps corresponding to intermediate energy levels between the bonding states and free-electron states. Unfortunately, due to difficulties in controlling crystal growth process at high temperatures, dislocations are a common type of crystallographic defect in SiC.[2] Along with extrinsic and intrinsic point defects governing recombination properties of SiC,[3] they also influence carrier transport properties of SiC epilayers such as carrier lifetime and diffusion length.[4,5] Since the major potential applications of SiC are high-power switching and microwave devices, where the carrier lifetime and diffusion length play a fundamental role, studying the effect of crystallographic defects on these parameters is of great interest.

The two major types of dislocations in hexagonal SiC are dislocations with the direction of dislocation line along $\langle 0001 \rangle$ (threading type) and $\langle 11\bar{2}0 \rangle$ (basal plane type). It was reported that basal plane dislocations can be significantly reduced in epitaxial layers by converting them into threading dislocations through "conversion epitaxial growth process."[6] However, the densities of threading screw dislocations (TSDs) and threading edge dislocations (TEDs) with Burgers vectors $c[0001]$ and $a1/3[11\bar{2}0]$, respectively (where c and a are lattice constants of hexagonal structure SiC), is still high. In good quality epitaxial films the density of threading dislocations reaches $\sim 10^3$ cm^{-2},[7,8] which represents a problem for SiC electronic devices. It was found that TSDs are detrimental for low-voltage *p*-*n* and high voltage Schottky diodes and their presence results in high reverse leakage current and low reverse breakdown voltage.[9,10] At the same time, the effect of TEDs on device performance is still unclear. Available experimental data regarding the electrical activity of TSDs and TEDs in SiC prove that both defects serve as efficient recombination sites degrading carrier transport properties of the material.[11–13] Since TSDs and TEDs have different core structures, different recombination properties of these defects can be expected. This was found in recent photoluminescence studies, which revealed different radiative recombination behavior of these defects.[14] However, the degree of impact of the specific dislocation type on carrier lifetime or diffusion length of SiC epitaxial films is still not established.[4,5] Also, no systematic theoretical investigations have been conducted for threading dislocations in SiC and the atomic and electronic structures of these defects are still not completely understood. One of the reasons for the limited amount of experimental work on this topic is the difficulty to access the recombination properties of the individual dislocations by using conventional characterization techniques such as photoluminescence, microwave photoconductivity decay, or transient-free carrier absorption, which are based on macroscopic rather than microscopic analysis of the material.[4,15,16]

In the present work, the electron beam induced current (EBIC) mode of a scanning electron microscope (SEM) was used to study the effect of threading screw and edge dislocations on the local minority carrier diffusion length in 4H–SiC epitaxial films and to aid in the understanding of recombination properties of these defects. Due to its high spatial resolution, down to submicron level,[17] and the possibility of measuring nonuniformity of diffusion lengths with high accuracy[18] in comparison with above mentioned techniques, EBIC is a powerful tool for visualization and characterization of electrically active defects in semiconductors.

[a)]Present address: Global Defense Technology & Systems, Inc., Crofton, Maryland 21114, USA. Electronic mail: serguei.maximenko.ctr.rs@nrl.navy.mil.

 © 2010 American Institute of Physics

Downloaded 08 Jul 2010 to 132.250.22.5. Redistribution subject to AIP license or copyright; see http://jap.aip.org/jap/copyright.jsp

Report Documentation Page

Form Approved
OMB No. 0704-0188

Public reporting burden for the collection of information is estimated to average 1 hour per response, including the time for reviewing instructions, searching existing data sources, gathering and maintaining the data needed, and completing and reviewing the collection of information. Send comments regarding this burden estimate or any other aspect of this collection of information, including suggestions for reducing this burden, to Washington Headquarters Services, Directorate for Information Operations and Reports, 1215 Jefferson Davis Highway, Suite 1204, Arlington VA 22202-4302. Respondents should be aware that notwithstanding any other provision of law, no person shall be subject to a penalty for failing to comply with a collection of information if it does not display a currently valid OMB control number.

1. REPORT DATE	2. REPORT TYPE	3. DATES COVERED
MAR 2010		**00-00-2010 to 00-00-2010**

4. TITLE AND SUBTITLE	
Effect of threading screw and edge dislocations on transport properties of 4H-SiC homoepitaxial layers	5a. CONTRACT NUMBER
	5b. GRANT NUMBER
	5c. PROGRAM ELEMENT NUMBER
6. AUTHOR(S)	5d. PROJECT NUMBER
	5e. TASK NUMBER
	5f. WORK UNIT NUMBER
7. PERFORMING ORGANIZATION NAME(S) AND ADDRESS(ES) **Naval Research Laboratory,4555 Overlook Avenue SW,Washington,DC,20375**	8. PERFORMING ORGANIZATION REPORT NUMBER
9. SPONSORING/MONITORING AGENCY NAME(S) AND ADDRESS(ES)	10. SPONSOR/MONITOR'S ACRONYM(S)
	11. SPONSOR/MONITOR'S REPORT NUMBER(S)

12. DISTRIBUTION/AVAILABILITY STATEMENT

Approved for public release; distribution unlimited

13. SUPPLEMENTARY NOTES

14. ABSTRACT

15. SUBJECT TERMS

16. SECURITY CLASSIFICATION OF:			17. LIMITATION OF ABSTRACT	18. NUMBER OF PAGES	19a. NAME OF RESPONSIBLE PERSON
a. REPORT	b. ABSTRACT	c. THIS PAGE			
unclassified	**unclassified**	**unclassified**	**Same as Report (SAR)**	**6**	

Standard Form 298 (Rev. 8-98)
Prescribed by ANSI Std Z39-18

II. EXPERIMENTAL PROCEDURE

A. Samples and characterization details

n-type 4H–SiC epitaxial films with thicknesses $\sim 20\ \mu$m, net doping concentration $\sim 8.6 \times 10^{14}$ and 1.1×10^{16} cm^{-3}, and dislocation densities $\sim 10^3$ cm^{-2} were used to study the recombination properties of threading dislocations. The epilayers were grown by hot-wall chemical vapor deposition (CVD) process on 4H–SiC (0001) wafers 8° off-cut toward the $\langle 11\bar{2}0 \rangle$ direction. Schottky contacts with diameters of 120 and 180 μm were fabricated using *e*-beam thin film deposition of Ti (100 Å thick) and then Ni (1000–1500 Å thick), followed by photolithography and rapid thermal annealing at 1000 °C for 5 min in a nitrogen atmosphere. No edge termination was employed. Prior to metal deposition, the sample surface was treated using a standard RCA cleaning procedure in order to remove organic and ionic contaminations from the surface. Ohmic contacts to the backside of the n^+ substrate were formed by blank *e*-beam deposition and annealing of a Ni film prior to Schottky contact formation.

EBIC studies were conducted in an LEO 435VP SEM using a constant beam current of 100 or 500 pA and an accelerating voltage in the range of 1–30 kV. EBIC intensity maps from Schottky structures were obtained by raster-scanning the *e*-beam across the sample and measuring the collected current as a function of *e*-beam position using a Keithley model 617 Electrometer. The experimental data were acquired and processed by means of a software developed by the authors using LABVIEW and MATHCAD. The *e*-beam current was monitored by a Faraday cup mounted on the SEM stage. Barrier height and doping concentration values needed for the calculation of the diffusion length were extracted from current-voltage (I-V) characteristics of the Schottky contacts using the thermoionic-field emission model[19] and from the capacitance-voltage (C-V) measurements. Deep level transient spectroscopy (DLTS) was used to estimate the density of $Z_{1/2}$ defects in the samples. Finally, after electrical characterization, preferential chemical etching of the samples in molten KOH at 500 °C for 15 min was performed to identify the nature of threading dislocations.[20]

B. Diffusion length calculation

To measure the minority carrier diffusion length in the vicinity of dislocations and defect free regions, we used the method proposed by Wu and Wittry,[18] which allows identification of diffusion length from the analysis of the collection efficiency of a Schottky barrier exposed to a stationary *e*-beam at variable accelerating voltages (Fig. 1). Unlike the conventionally used linescan method formulated by Joannou and Davidson,[21] this approach allows local measurement of the diffusion length, L, at the particular point of interest within the area occluded by the Schottky contact. The dislocation can be described as a cylindrical region with radius r with reduced minority carrier lifetime τ' (in contrast to the lifetime τ of the surrounding material), characterized by capture cross section σ, (Fig. 1) (Ref. 22) and related to the measured diffusion length by $L=\sqrt{D\tau}$, where D is the diffusion coefficient.

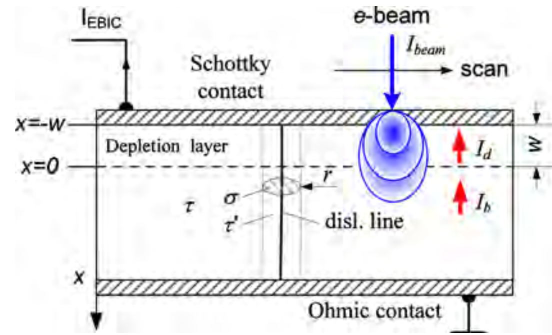

FIG. 1. (Color online) Schematic of the EBIC model used in this work for diffusion length measurements.

The total current generated by *e*-beam and collected by the Schottky barrier (I_{EBIC}) is composed of charges collected from the depletion (I_d) and quasineutral (I_b) regions of the device, and in the case of *n*-type material, is given by

$$I_d = -q\int_{-w}^{0} g(x)dx, \quad I_b = -qD_p(wL_p)^{-1} \left. \frac{d\Delta p}{dx} \right|_{x=0}, \tag{1}$$

where Δp is the excess carrier density, $g(x)$ is the distribution of generation volume function of electron-hole pairs excited by the *e*-beam, q is the electron charge, and w is the depletion layer width. The Wittry model assumes that recombination within the depletion region and at the metal-semiconductor interface of the Schottky contact is negligible. Also, 100% collection of carriers diffused from the quasineutral region is assumed at the boundary of the space charge region. The charge collection efficiency of the barrier is expressed as

$$\eta = I_{\text{EBIC}}/qG = E_{\text{ehp}}(I_b + I_d)/[I_{\text{beam}}E(1-f)], \tag{2}$$

where G is the generation rate of electron-hole pairs excited by the *e*-beam per unit volume. E_{ehp} represents the mean energy to create one electron-hole pair which can be found as $E_{\text{ehp}} = 2.1 \times E_g + 1.3$ [where E_g is the band gap of the material (for 4H–SiC 3.26 eV)], I_{beam} is the beam current, and E is the electron beam energy. The units of E_g, I_{beam}, and E are eV, A, and eV, respectively. Parameter f represents the fractional electron beam energy loss due to the backscattering of incident electrons (equal to 0.07 for SiC and constant for all accelerating voltages[5]).

The experimental collection efficiency is obtained by measuring I_{EBIC} as a function of *e*-beam accelerating voltage, while the theoretical collection efficiency is derived substituting measured I_{EBIC} in Eq. (2) by calculated I_d and I_b from Eq. (1). By curve-fitting of the theoretical curve to experimental values of η by L, the diffusion length in the vicinity of dislocations and defect free regions is evaluated. Additional parameters involved in curve-fitting are carrier concentration of semiconductor, the thickness of Schottky metal contact and Schottky barrier height. Their degree of magni-

Downloaded 08 Jul 2010 to 132.250.22.5. Redistribution subject to AIP license or copyright; see http://jap.aip.org/jap/copyright.jsp

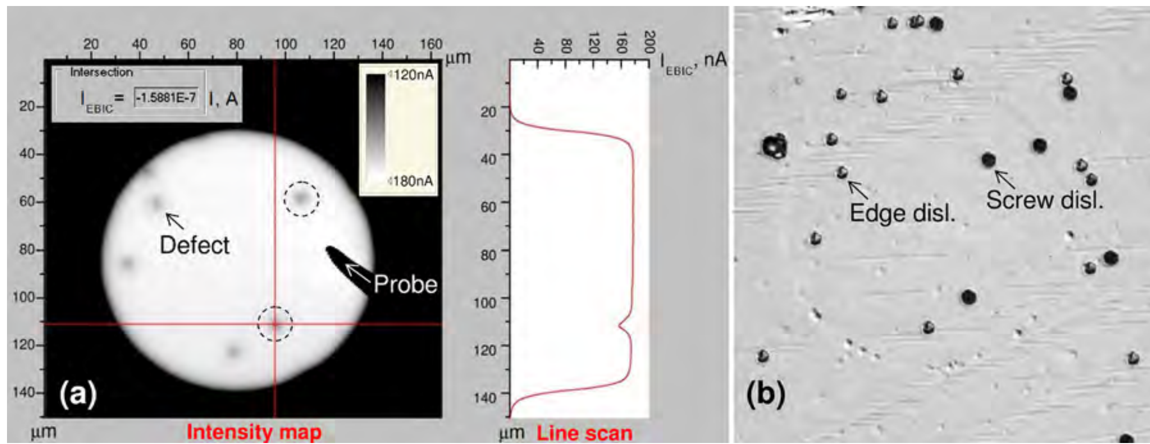

FIG. 2. (Color online) (a) EBIC intensity map acquired at 30 kV from a Schottky contact on an intentionally n-doped epilayer (1.1×10^{16} cm^{-3}) and (b) corresponding Nomarski optical image after preferential molten KOH etching.

tude can be rather precisely determined using other characterization techniques (I-V, C-V, etc.), though with not so high spatial resolution.

III. RESULTS AND DISCUSSION

Figure 2(a) shows a typical two dimensional EBIC intensity map of a Schottky contact obtained at 30 kV accelerating voltage from one of our samples. The bright region represents the Schottky contact, where the carriers generated by the e-beam are collected by the space charge region of the device, thus producing EBIC current. The dark, circular shaped features within the contact area are related to a local decrease in the EBIC current due to enhanced carrier recombination, and represent typical EBIC signatures of threading screw or edge dislocations in SiC. Figure 2(b) shows the optical image of the same region as in Fig. 2(a), obtained after removal of the Schottky contact and chemical etching of the sample in molten KOH in order to reveal the location of the dislocations and their type. Threading dislocations are revealed by characteristic etch pit shapes. TSDs exhibit larger and deeper etch pits than the TEDs (see Fig. 3), which allows identification of the treading dislocation type in SiC.[23] It can be seen from Fig. 2 that there is a one-to-one correlation between etch pits and defects revealed by EBIC. Using the etch pit map in Fig. 2(b), all screw dislocations in the EBIC intensity map were marked by circles [see Fig. 2(a)].

An EBIC line scan across one of the dislocations is shown in Fig. 2(a). The maximum drop in EBIC current occurs at the dislocation core[24] and defines the maximum EBIC contrast of dislocation by $c_{\max}=1-I_{\text{def. min}}/I_{\text{def. free}}$, where $I_{\text{def. min}}$ is the current collected at the center of dislocation core and $I_{\text{def. free}}$ is the current collected far away from defect. Since 100% collection efficiency is usually assumed within the depletion region, it is clear that the EBIC contrast

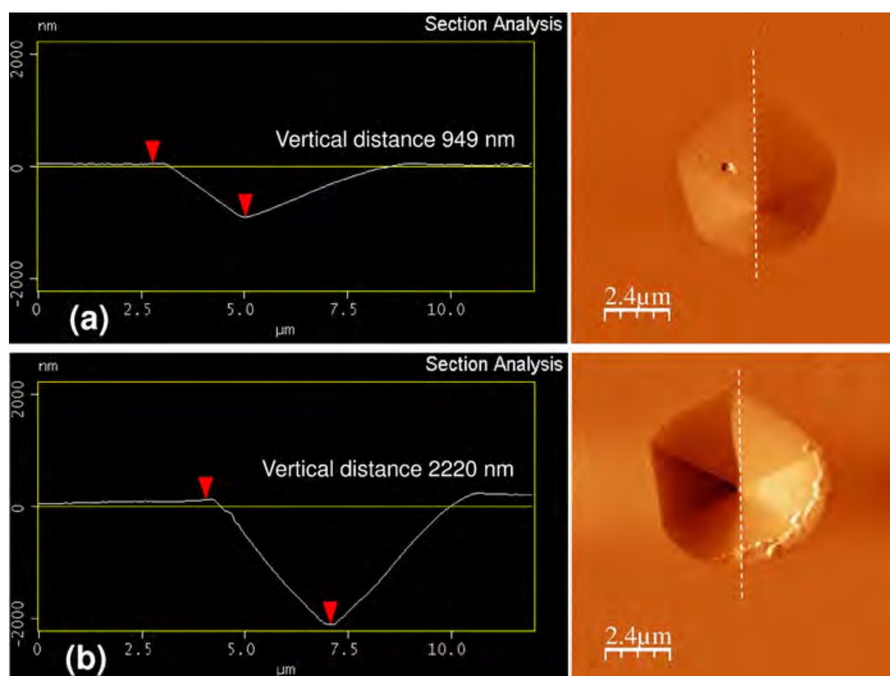

FIG. 3. (Color online) AFM images and cross sectional surface profiles of etch pits from threading (a) edge and (b) screw dislocations.

Downloaded 08 Jul 2010 to 132.250.22.5. Redistribution subject to AIP license or copyright; see http://jap.aip.org/jap/copyright.jsp

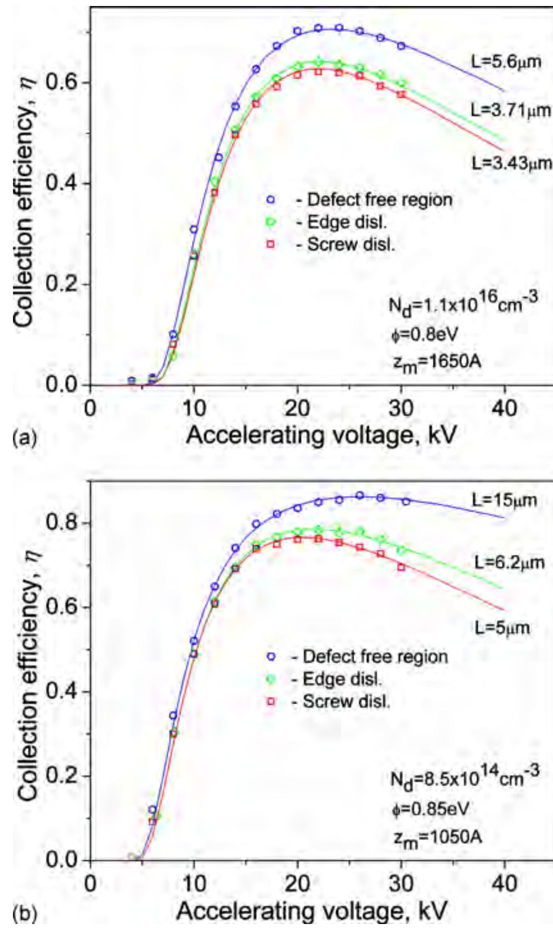

FIG. 4. (Color online) Collection efficiencies as a function of *e*-beam accelerating voltage measured for samples with (a) $N_d = 1.1 \times 10^{16}$ cm^{-3} and (b) $N_d = 4.5 \times 10^{14}$ cm^{-3} at screw, edge, and dislocation free regions. Symbols and solid lines represent experimental data and theoretical calculations, respectively.

of the dislocation originates entirely from the quasineutral region of the Schottky contact.

In order to reveal the difference in recombination activity of screw and edge dislocations, we determined charge collection efficiency of individual TEDs and TSDs in our samples at varying *e*-beam accelerating voltages. Figure 4 shows typical collection efficiency curves for TSD, TED, and defect free regions obtained experimentally and calculated theoretically using the values of the thickness of metal contact (z_m), Schottky barrier height (ϕ) and carrier concentration (N_d) shown in Fig. 4. Although the experimental results agree fairly well with our theoretical calculations, the experimental collection efficiency values measured at dislocations in the range 15 to 25 kV accelerating voltages have slight deviation toward lower values. Similar disagreement of the theory with experiment for low accelerating voltages was reported by other researchers.[18,25,26] It was suggested that the observed reduction in the collection efficiency is related to recombination within the space charge region and the metal-semiconductor interface. However, detailed calculations of the collection efficiency in the presence of Shockley–Read–Hall recombination, at the metal-semiconductor interface, showed that the current loss is negligible even for high values of recombination rate at the metal-semiconductor interface of the Schottky contact. Therefore, it was concluded that low experimental values of collection efficiency could be related to the loss of carriers in the depletion region of the device due to recombination or some additional mechanisms.[25]

Diffusion lengths of the minority carriers in the defect free regions, found from EBIC measurements, were ~15 and 5.4 μm, for low (8.6×10^{14} cm^{-3}) and moderately doped (1.1×10^{16} cm^{-3}) samples, respectively. The variation in the diffusion lengths for these samples can be explained by the large difference in the concentration of $Z_{1/2}$ defects revealed by DLTS measurements ($n_{Z1/2} = 4.46 \times 10^{13}$ cm^{-3} in moderately doped sample versus $n_{Z1/2} = 1.05 \times 10^{12}$ cm^{-3} in low doped sample). Since the $Z_{1/2}$ defect is the major lifetime limiting point defect in 4H–SiC epitaxial layers,[3,27] the difference in its concentration is believed to be responsible for different diffusion lengths in the two samples. In both samples, screw and edge dislocations serve as efficient recombination sites, strongly decreasing the diffusion length of material in the vicinity of dislocations. However, screw dislocations show consistently shorter diffusion lengths, suggesting stronger recombination activity than edge dislocations, as can be clearly seen from the graphs in Fig. 4. While the obtained diffusion length values give an idea about the recombination activity of dislocations, it is more convenient to use the concept of defect recombination strength (γ) (Ref. 28) to reflect the recombination efficiency of the individual dislocations. For the dislocation with the dislocation line perpendicular to the Schottky barrier, the recombination strength is given by $\gamma = \sigma D_p^{-1}(1/\tau' - 1/\tau) \Rightarrow \sigma(1/L'^2 - 1/L^2)$.[29] Considering for simplicity similar dimensions of capture cross sections of dislocation cores for TED and TSD, the relative defect recombination strength can be expressed as $(1/L'^2 - 1/L^2)$. The defect recombination strength has a straightforward relationship to the EBIC contrast according to $c = \gamma \cdot F(R_e, L)$, where F is a correction factor depending on the electron penetration range (R_e) and diffusion length of the surrounding defect free region.[29] Based on this, by analyzing the contrast from dislocations at similar excitation conditions, it is possible to estimate and differentiate defects with variable recombination strengths.

Table I summarizes the calculated relative recombination strength and the maximum EBIC contrast values obtained for threading screw and edge dislocations in low and moderately doped samples. It can be clearly seen from Table I that screw dislocations have higher recombination efficiency than edge dislocations. The measured EBIC contrast of defects at 30 kV accelerating voltage is in good agreement with calculated relative recombination strength values, meaning that higher recombination strength corresponds to higher EBIC contrast. Thus, all the studied screw dislocations always exhibited the highest magnitude of EBIC contrast. This allowed us to distinguish TEDs from TSDs using only the EBIC intensity maps of defects. As an example, Fig. 5 shows an EBIC intensity map obtained from Fig. 2(a) by adjusting the *min* and *max* of the EBIC intensity scale to optimize the screw dislocations contrast and saturate the other defects. Thus, this approach allows nondestructive identification of the dislocation type in Schottky, and probably most other SiC device struc-

Downloaded 08 Jul 2010 to 132.250.22.5. Redistribution subject to AIP license or copyright; see http://jap.aip.org/jap/copyright.jsp

TABLE I. Summary of recombination properties of screw and edge dislocations in the samples.

	Diffusion length (μm)		Relative recombination strength, $(1/L'^2-1/L^2)$		EBIC contrast, c_{max} (%)	
	Dislocation type		Dislocation type		Dislocation type	
Sample	Edge	Screw	Edge	Screw	Edge	Screw
$N_d=8.6\times10^{14}$ cm^{-3}	6.2	5	0.022	0.036	10.5	13.7
$N_d=1.1\times10^{16}$ cm^{-3}	3.71	3.43	0.033	0.045	10.9	12.9

tures, using EBIC. Note that for defects with similar recombination strengths (e.g., TEDs and TSDs in this study), it is convenient to measure the dislocation contrast at higher accelerating voltages due to the larger width of the intensity profile of the defect,[24] which allows the contrast measurement error to be minimized at the center of a dislocation core and to conduct experimental measurements at lower magnification. Also, at higher accelerating voltages the difference observed in charge collection efficiencies of defects with similar recombination strength is more pronounced, as clearly seen in Fig. 4.

In order to better understand recombination properties of dislocations in 4H–SiC, we conducted temperature dependent studies of the dislocation EBIC contrast. Figure 6 shows typical experimental dependences of EBIC contrast on temperature, in the range of 5–300 K, for edge and screw dislocations measured with identical conditions in the low doped sample. As shown in Fig. 6, both types of dislocations have similar contrast behavior. At temperatures below 30 K, the contrast at the dislocations was below the detection limit of our system. The fast rise of the contrast at about 50 K followed by monotonic contrast increase with temperature is seen. Similar contrast behavior was observed from dislocations in Si.[30] It was demonstrated that such contrast behavior occurs when recombination at dislocations is controlled by deep centers.[31] Moreover, modeling results indicate that such dependence of EBIC contrast with temperature in silicon is governed by electron-hole pair recombination via shallow dislocation bands, probably introduced by the strain field of the defect and the deep levels in the vicinity of the dislocation core, attributed to impurity atoms segregated at the dislocation core. The similarity of the contrast versus temperature behavior in our case compared to that reported in Ref. 30 suggests that deep levels at dislocations are responsible for the recombination activity of the TEDs and TSDs in the studied epitaxial layers. In the case of SiC, it is not clear whether the deep levels at the dislocation are intrinsic or introduced by impurities segregated at dislocations, which are attracted by the dislocation's strain fields. Since screw and edge dislocations have different strain field it can be expected distinct dislocation-impurity interaction behavior. Particularly, it was shown that the distance at which the impurity atoms are captured by dislocations is significantly larger for screw type dislocations than for edge dislocations (i.e., $R_s/R_e\sim3.3$, where R_s and R_e are the "effective capture radius" for the screw and edge dislocations).[32] This can result in change in the electronic properties of dislocations and nearby surrounding regions cause by gettering effect or the formation of the Cottrell atmosphere.[33,34]

Calculations of atomic and electronic structures of threading dislocations in Wurtzite GaN (Refs. 35 and 36) (a wide band gap semiconductor with lattice structure similar to that of 4H–SiC), showed that TSDs introduce more states in the band gap in comparison with edge dislocations and their recombination activity is presumably stronger than that of edge dislocations, which corroborates our experimental observations. Modeling of the electronic properties of clean dislocations and dislocations decorated by specific impurities in SiC is expected to shed more light on this problem.

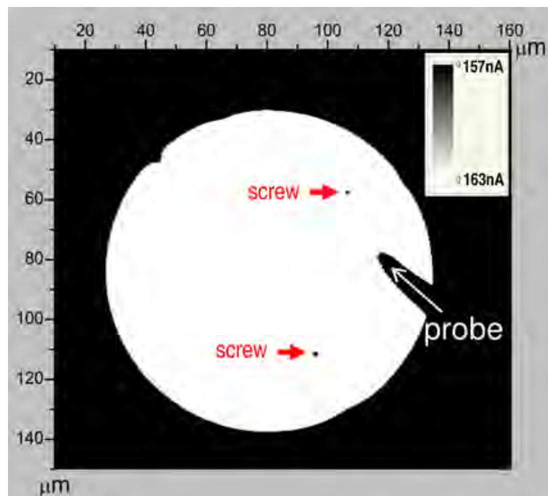

FIG. 5. (Color online) EBIC image of Schottky contact with enhanced contrast to reveal defects with strongest contrast.

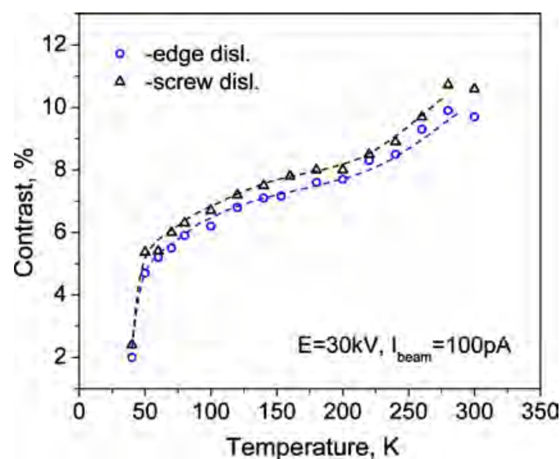

FIG. 6. (Color online) Dependence of the dislocation contrast on temperature. Fitting results are presented by dashed lines.

Downloaded 08 Jul 2010 to 132.250.22.5. Redistribution subject to AIP license or copyright; see http://jap.aip.org/jap/copyright.jsp

IV. SUMMARY AND CONCLUSIONS

In this work, EBIC was used to characterize threading edge and screw dislocations in *n*-type 4H–SiC epitaxial layers. Particularly, dislocation-related characteristics such as minority carrier diffusion length, EBIC contrast and its temperature dependence and relative recombination strength was measured in the epitaxial layers with doping concentrations of $\sim 8.6\times 10^{14}$ and 1.1×10^{16} cm^{-3}. Our results clearly show that screw and edge dislocations have different recombination activity in SiC. The relative recombination strength of screw dislocations was up to 40% larger than that of edge dislocations, depending on the doping concentration of the epitaxial layer. The measurements of minority diffusion length revealed that the reduction in diffusion length is stronger in the vicinity of screw dislocations than that of edge dislocations. Based on the character of temperature dependence of the EBIC contrast, we suggest that recombination activity of TEDs and TSDs in SiC is controlled by deep level centers in the vicinity of the dislocation core. It was shown that EBIC contrast of screw dislocations can be up to 30% larger that that of the edge dislocation, which makes it possible to distinguish between threading screw and edge dislocations in SiC epilayers using EBIC. This result has high practical importance for nondestructive characterization of SiC device structures and for defect-device correlation studies.

ACKNOWLEDGMENTS

The authors are thankful to Dr. P. B. Klein for useful discussion and valuable suggestions during manuscript preparation. S. I. Maximenko acknowledges support of this research provided by the NRC program at NRL. B. L. VanMil and K. K. Lew acknowledge the support of the American Society for Engineering Education Postdoctoral Fellowship Program at NRL.

[1]W. Shockley, Phys. Rev. **91**, 228 (1953).
[2]T. Sudarshan and S. I. Maximenko, Microelectron. Eng. **83**, 155 (2006).
[3]P. B. Klein, Phys. Status Solidi A **206**, 2257 (2009).
[4]J. Hassan and J. P. Bergman, J. Appl. Phys. **105**, 123518 (2009).
[5]M. Tabib-Azar, S. M. Hubbard, and C. M. Schnabel, J. Appl. Phys. **84**, 3986 (1998).
[6]R. E. Stahlbush, B. L. VanMil, R. L. Myers-Ward, K.-K. Lew, D. K. Gaskill, and C. R. Eddy, Jr., Appl. Phys. Lett. **94**, 041916 (2009).
[7]Y. Chen, N. Zhang, X. R. Huang, D. R. Black, and M. Dudley, Mater. Sci. Forum **600–603**, 301 (2009).
[8]E. Berkman, R. T. Leonard, M. J. Paisley, Y. Khlebnikov, M. J. O'Loughlin, A. A. Burk, A. R. Powell, D. P. Malta, E. Deyneka, M. F. Brady, I. Khlebnikov, V. F. Tsvetkov, H. M. Hobgood, J. Sumakeris, C. Basceri, V. Balakrishna, C. H. Carter, Jr., and C. Balkas, Mater. Sci. Forum **615–617**, 3 (2009).
[9]P. Neudeck, IEEE Trans. Electron Devices **46**, 478 (1999).
[10]Q. Wahab, A. Ellison, A. Henry, E. Janzén, C. Hallin, J. Di Persio, and R. Martinez, Appl. Phys. Lett. **76**, 2725 (2000).
[11]C. M. Schnabel, M. Tabib-Azar, P. G. Neudeck, S. G. Bailey, H. B. Su, M. Dudley, and R. P. Raffaelle, Mater. Sci. Forum **338–342**, 489 (2000).
[12]B. J. Skromme, K. C. Palle, M. K. Mikhov, H. Meidia, S. Mahajan, X. R. Huang, W. M. Vetter, M. Dudley, K. Moore, S. Smith, and T. Gehoski, Mater. Res. Soc. Symp. Proc. **742**, K3.4.1 (2003).
[13]C. Díaz-Guerra and J. Piqueras, J. Phys.: Condens. Matter **16**, S217 (2004).
[14]K. X. Liu, X. Zhang, R. E. Stahlbush, M. Skowronski, and J. D. Caldwel, Mater. Sci. Forum **600–603**, 345 (2009).
[15]M. Kato, M. Kawa, T. Mori, M. Ichimura, S. Sumie, and H. Hashizume, Jpn. J. Appl. Phys., Part 1 **46**, 5057 (2007).
[16]V. Grivickas, A. Galeckas, V. Bikbajevas, J. Linnros, and J. A. Tellefsen, Thin Solid Films **364**, 181 (2000).
[17]C. E. Norman, Solid State Phenom. **78–79**, 19 (2001).
[18]C. J. Wu and D. B. Witty, J. Appl. Phys. **49**, 2827 (1978).
[19]F. A. Padovani and R. Stratton, Solid-State Electron. **9**, 695 (1966).
[20]R. Yakimova, A.-L. Hylén, M. Tuominen, M. Syväjärvi, and E. Janzén, Diamond Relat. Mater. **6**, 1456 (1997).
[21]D. E. Ioannou and S. M. Davidson, J. Phys. D: Appl. Phys. **12**, 1339 (1979).
[22]P. R. Wilshaw, T. S. Fell, and G. R. Booker, in *Point and Extended Defects in Semiconductors*, edited by G. Benedek, A. Cavallini, and W. Schröter (Plenum, New York, 1989), p. 243.
[23]S. Ha, Mater. Sci. Forum **389–393**, 443 (2002).
[24]C. Donolato, Appl. Phys. Lett. **34**, 80 (1979).
[25]B. Sieber and P. Carton, Phys. Status Solidi A **127**, 423 (1991).
[26]Y. Beggah, D. E. Mekki, N. Tabet, and R. J. Tarento, Solid-State Electron. **42**, 379 (1998).
[27]K. Danno, D. Nakamura, and T. Kimoto, Appl. Phys. Lett. **90**, 202109 (2007).
[28]C. Donolato, Optik (Stuttgart) **52**, 19 (1978/79).
[29]M. Kittler and W. Seifert, Cryst. Res. Technol. **16**, 157 (1981).
[30]V. Kveder, M. Kittler, and W. Schröter, Phys. Rev. B **63**, 115208 (2001).
[31]M. Kittler and W. Seifert, Mater. Sci. Eng., B **24**, 78 (1994).
[32]F. S. Ham, J. Appl. Phys. **30**, 915 (1959).
[33]B. Pichaud, G. Mariani-Regula, and E. B. Yakimov, Mater. Sci. Eng., B **71**, 272 (2000).
[34]K. Sumino, Phys. Status Solidi A **171**, 111 (1999).
[35]A. T. Blumenau, J. Elsner, R. Jones, M. I. Heggieggie, S. Oberg, T. Frauenheim, and P. R. Briddon, J. Phys.: Condens. Matter **12**, 10223 (2000).
[36]A. T. Blumenau, C. J. Fall, J. Elsner, R. Jones, M. I. Heggie, and T. Frauenheim, Phys. Status Solidi C **0**, 1684 (2003).

Downloaded 08 Jul 2010 to 132.250.22.5. Redistribution subject to AIP license or copyright; see http://jap.aip.org/jap/copyright.jsp